



Preparation and optimization of silibinin-loaded chitosan-fucoidan hydrogel: An *in vivo* evaluation of skin protection against UVB

Masood Ali karami , Behzad Sharif Makhmalzadeh , Mahsa Pooranian & Anahita Rezai

To cite this article: Masood Ali karami , Behzad Sharif Makhmalzadeh , Mahsa Pooranian & Anahita Rezai (2020): Preparation and optimization of silibinin-loaded chitosan-fucoidan hydrogel: An *in vivo* evaluation of skin protection against UVB, Pharmaceutical Development and Technology, DOI: [10.1080/10837450.2020.1856871](https://doi.org/10.1080/10837450.2020.1856871)

To link to this article: <https://doi.org/10.1080/10837450.2020.1856871>



Accepted author version posted online: 01 Dec 2020.



Submit your article to this journal [↗](#)



View related articles [↗](#)



View Crossmark data [↗](#)

Preparation and optimization of silibinin-loaded chitosan-fucoidan hydrogel: An *in vivo* evaluation of skin protection against UVB

Authors: Masood Ali karami¹, Behzad Sharif Makhmalzadeh^{1,2,*}, Mahsa Pooranian¹, Anahita Rezaei³

¹ Department of Pharmaceutics, School of Pharmacy, Ahvaz Jundishapur University of Medical Sciences, Ahvaz, Iran.

² Nanotechnology Research Center, Ahvaz Jundishapur University of Medical Sciences, Ahvaz, Iran

³ Department of pathobiology, faculty of veterinary medicine, shahidchamran University of Ahvaz, Ahvaz, Iran

* Correspondence: Behzad Sharif Makhmalzadeh; Nanotechnology Research Centre, Ahvaz Jundishapur University of Medical Sciences, Ahvaz, Iran; Email: makhmalzadeh@yahoo.com; <https://orcid.org/0000-0002-1441-3127>. Tel: +98-61-33738380

Abstract

Purpose: The objective of this study was to develop silibinin-loaded hydrogel for skin protection against UVB damage.

Method: Physical grafting was used to prepare hydrogel based on chitosan-fucoidan. Then, hydrogel properties, such as swelling, drug release rates, morphology, and structure, were evaluated to determine the optimum hydrogel for *in vivo* studies. In *in vivo* experiments, the silibinin permeability parameters were investigated through normal and UV-irradiated skin, anti-inflammatory property, and antioxidant effects after application of optimum hydrogel.

Results: The silibinin completely dispersed in the hydrogel, and FT-IR results showed that silibinin reacted with the chitosan and fucoidan and demonstrated a slow release pattern. The 50% and less than 70% of the drug-loaded on hydrogel were passed through normal and irradiated skin after 48 h, respectively. *In vivo* studies showed the effectiveness of optimized hydrogel in preventing the production of oxidative species and H₂O₂ after UVB radiation. Histological studies have shown that silibinin-loaded optimized hydrogel can prevent the hyperkeratosis, acanthosis, and infiltration of neutrophils into the dermis by UVB.

Conclusion: Optimized hydrogel effectively reduced the inflammation mediators interleukin-22 and TNF- α , which signify tissue destruction. Therefore, silibinin-loaded hydrogel can be introduced as an effective sun-protective product.

Keywords: silibinin, hydrogel, fucoidan, chitosan, chemopreventive agent, UVB-induced skin damage

Introduction

The human skin is the most vital aspect of the defense mechanism protecting the underlying tissues from the harsh external environment. Solar ultraviolet radiation (UV) is one of the most frequent factors that can cause serious disorders of the skin. UVA (315-400 nm) and UVB (280-315 nm) can reach the surface of the earth and adversely affect human health (Gonzaga 2009; Cavinat et al. 2017). UVA is responsible for immediate pigment darkening, which disappears within two hours and has chronic effects similar to those of UVB (Gonzaga 2009). Particularly UVB, due to its high energy, can cross the epidermis and reach the upper dermis, where it interacts with cellular chromosomes, leading to DNA damage and increased oxidative stress. Chronic exposure of the skin to UVB causes skin aging, which is characterized by skin fragility, laxity, roughness, dryness, hyper-pigmentation, blister formation, a leathery appearance, and formation of wrinkles and hyperkeratosis (Mohamed et al. 2014). Efficient skin protection methods can prevent the harmful effects of UVA and UVB.

Silibinin (SB) is a potent and principal component of silymarin extracted from *Silymarium* (Milk thistle). SB is a secondary alpha-hydroxy ketone (Fig 1) and the main polyphenolic biologically active constituent found in Milk thistle (approximately 50-70%). SB has beneficial effects for inhibiting UVB-induced skin injuries (Marchiori et al. 2017). Studies have shown that the dietary feeding of silibinin provides strong protection against UVB-induced damage to the skin either by (a) either preventing DNA damage or enhancing repair; (b) reducing the UVB-induced hyper-proliferative response; and (c) inhibiting UVB-caused apoptosis and sunburn cell formation, possibly via the SB-caused upregulation of p53 and p21/cip1 as major UVB damage control sensors (Dhannalakshmi et al. 2005). Unfortunately, SB has low bioavailability due to its degradation in gastric fluid, low water solubility, and poor enteral absorption (Zhao et al. 2016).

Therefore, it seems that the topical application of SB could be a new opportunity for skin protection against UVB radiation.

Hydrogel is a swellable three-dimensional network formed by cross-linking polymer chains. Hydrogels can be used for a wide range of applications, such as in controlled drug delivery systems (DDSs) and as specialized carriers for various macromolecules. Hydrogels protect drugs from hostile environments and can control drug release by changing the gel structure in response to environmental stimuli (Qiu & Park 2001). Hydrogel possesses stronger spreadability and stability and exhibits a better drug-controlled release pattern than other semi-solid preparations. Hydrogels demonstrate more advantages as topical drug delivery systems, such as a degree of flexibility similar to natural tissue, and they act as drug depots in the skin.

Natural polymers, such as polysaccharides and proteins, have also been used as the structural material in hydrogels. This is largely due to the current interest in the intrinsic properties of these polymers, including biocompatibility, low toxicity, and susceptibility to enzymatic degradation. Among these polymers, polysaccharides do not demonstrate disadvantages, such as immunogenicity and the potential risk of transmitting animal-derived pathogens. These attractive natural polysaccharides share the benefits of other natural polymers but do not induce an immune response. Chitosan is a very well-known polysaccharide (Fig 1) that has been used for hydrogel formation. Hydrogels composed of chitosan alone or in combination with alginate, methylcellulose, or carbopol have been used as drug delivery systems (Dai et al. 2008; Badek et al. 2000).

Fucoidan, a sulfated polysaccharide (Fig 1) extracted from brown algae, was first isolated by Kylin almost a century ago and was found to contain a significant amount of L-fucose and sulfate ester groups. Recently, fucoidan has been studied extensively due to potential anti-tumor, anti-

viral, anti-complement, and anti-inflammatory activities (Bhattarai et al. 2010). Fucoidan is a sulfated polysaccharide, and its photo-protective effects against UVB have been investigated. Fucoidan inhibits UVB-induced MMP-1 expression in human skin by inhibiting the ERK pathways (Moon et al. 2008). Therefore, the novelty of this study is that a marine natural-based vehicle with sun-protective properties is prepared for the delivery of SB as a natural UV-protective agent. In this study, a hydrogel composed of chitosan and fucoidan was used as a silibinin topical delivery system to protect the skin against UVB.

Insert fig 1. **Materials and Methods**

Materials

Silibinin, Fucoidan, chitosan, diamino-benzidine were purchased from Sigma-Aldrich, lactic acid, N-Butanol, and potassium monobasic were purchased from Samchum (South Korea), DMSO, Tris-buffer, dodecyl sulfate, and methyl green have been purchased of Merck (Germany). Trademark[®] sun-protective cream was provided by Cinere (Cosmetic Company, Tehran, Iran).

Methods

Experimental design and optimization

Several parameters could affect final hydrogel properties and its permeability through the UVB-irradiated skin. Therefore full-factorial design was used concerning two independent variables at three levels in this study for experimental design. Major variables in the determination of

hydrogel's properties were chitosan and Fucoïdan percentage. Nine different formulations with low and high values of Chitosan percentage (1 %, 2%, and 4%), Fucoïdan percentage (0/1%,0/2 %, and 0/4%), and 100 µM SB were prepared and their properties such as porosity, hydrogel swelling ratio and morphology, drug release, and permeation parameters through mice skin were evaluated (Sezer et al. 2008). Optimization was done based on a checkpoint analysis and performed with Minitab 16 software to find the level of independent variables that would obtain a maximum value of swelling ratio after 60 min and the maximum amount of % drug release after 1 h (% R₁). Swelling ratio and % drug release are critical parameters that determine SB concentration into the skin as the main site for protection against UV-B.

Preparation of Hydrogels

Fucoïdan was dissolved in a 1% w/v lactic acid solution contained 0.2% Span 20 by mechanical shaking at 300rpm for 1h. Then chitosan was added to swell in the fucoïdan solution, SB with different concentration (0.048, 0.12, and 0.22 mg/g equal to 100, 250, and 450 µmol/l) added with agitation, and then 0.5% w/v glutaraldehyde was added as a crosslinker agent and left overnight to prepare hydrogels. Hydrogels were kept at 4°C (Qiu & Park. 2001). The uniformity of drug in the hydrogel was investigated by the drug content uniformity test described in the next experiment.

SB content and pH of hydrogels

1 g SB-loaded hydrogel was dissolved in 100 ml of buffer phosphate (pH= 7) including 0.3% span 20. The obtained solution was filtered through a Millipore filter (0.45 µm) and then the SB

content estimated by HPLC method (Baviskar et al., 2013). The experiment repeated triplicated and SB content reported as mean \pm sd.

1 g SB-loaded hydrogel was weighed and mixed with 20 ml of purified water and then the pH was measured by pH meter (Corning, USA).

Spreadability measurement

For this purpose, 1 g SB-loaded hydrogel was pressed between two plates (15 \times 15 cm) by putting 5 g standardized weight on the upper plate. After 5 minutes diameter of the spread circle was measured and reported as spreadability value (Rao et al., 2009).

Rheology measurement

The rheology of hydrogels was performed by a cone and plate viscometer (Thermo Scientific, Germany) at 32 °C (diameter 20 mm; cone angle 1°). Viscosity was measured at shear rate 0.1-200 s⁻¹ over 250 sec (Cuomo et al., 2019).

Swelling Study

The swelling studies were carried out gravimetrically in pH 7.4 phosphate buffer (PBS).

One gram hydrogel was put in a petri dish and 10ml of PBS (pH 7.4) was added until the hydrogels reached the constant weight at 25°C. At predetermined time intervals, the hydrogels blotted with the filter paper to remove excess water and reweighed. Each experiment was performed in triplicate. The swelling ratio (Ds) was calculated using Eq. 1.

$$D_s = \frac{W_t - W_0}{W_t} \times 100 \quad \text{Eq.1}$$

Where W_t is the weight of hydrated gel at time t , W_0 is the initial weight of the gel (Qiu & Park, 2001).

Characterization of the hydrogel by FT-IR

The nature of the interacting forces can be changed during the gelation process. This can be observed with a Fourier transform infrared spectroscopy (FT-IR). FT-IR spectra were recorded on an FTIR spectrometer (Uker, Vertex70, and Germany) at room temperature. Hydrogel samples were dried under atmospheric conditions for 24 h. Chitosan, Fucoidan, SB, and the dried hydrogel with SB and without SB were triturated with KBr in the ratio of 1:100 and pressed to form pellet samples and their spectra were prepared in the range of 400–4000 cm^{-1} (Badek et al. 2000).

Differential scanning calorimetry (DSC)

The thermal properties of SB-loaded optimal hydrogel and pure SB were examined using DSC (Mettler DSC 30, Mettler-Toledo, OH, USA). The samples were placed in aluminum pans, and in a heating program, the temperature was increased to 200 $^{\circ}\text{C}$ (heating rate: 5 $^{\circ}\text{C}/\text{min}$) (Marchiori et al. 2017).

In-vitro Drug release

Drug release profiles were performed by static diffusion cells with a thermo-regulated water jacket and the temperature was maintained at 37 °C. The donor and receptor phases were separated by the acetate cellulose (Spectra/Por, molecular weight cut of 3000–4000 Da) membrane. To achieve solvent equilibrium between donor and receptor phases, the donor and receptor chambers were filled with receptor phase and left for 1 h, and then the receptor phase was removed from the donor chamber and replaced with 5 g of 100 µmol/L SB- loaded hydrogel. 30 ml of buffer phosphate (pH= 7) including 0.3% Sorbitanmonolaurate (span 20) was used as the receptor phase to obtain sink condition. Samples were picked up in determined intervals over 48hrs, and the amount of SB released was determined by the HPLC method. The percentage of drug release after 1 (%R1), and 48 h (%R48) were determined as signs of burst and sustained release. The drug release mechanism was evaluated by fitting different models and calculating the correlation coefficient (R^2). In this experiment, an aqueous suspension of SB with the same concentration was used as control. Also, an *In vitro* release experiment was performed for optimized hydrogel contained 100, 250, and 450 µmol/L SB.

The Ex-vivo skin permeation studies

Dorsal skin was separated from newly sacrificed mice with ketamine. The subcutaneous fat was completely removed by cold acetone and stored at -20°C. The full-skin thickness was measured by digital micrometer (AAOC, France). The frozen skin was kept at room temperature to carry out the permeability experiment. An electrical conductor at 300 Hz was used for skin integrity evaluation by two stainless steel electrodes. Skin samples with the electrical resistance of more

than 3.9 KΩ/cm² were used in skin permeation experiments (Davies et al., 2014). The in-vitro skin permeation studies were performed using vertical glass diffusion cells fabricated in house with an effective diffusion area of approximately 1.53 cm². The volume of the receptor section was 10ml. The hydrated skin was mounted between the donor and receptor compartments of the cell without any damage due to the diffusion cell apparatus. The receptor medium was filled with Buffer phosphate including 0.3% Span 20 to obtain sink condition and constantly stirred using the externally driven magnetic beads at 37 °C and 300 rpm throughout the experiment. At each interval times (0.5, 1, 2, 4, 6, 8, 24, 28, 48 h), a 2 ml sample was withdrawn from the receptor medium and immediately replaced with an equivalent volume of Fresh Buffer including Span 20. The permeated amount of SB was determined using the HPLC method (Makhmal Zadeh et al. 2018). The results were plotted as cumulative permeated drug percent versus time. Based on these plots, the apparent permeability coefficient (Eq.2) and the steady-state permeation flux (J_{ss}) (Eq.3) were calculated.

$$P_{app} = \frac{dQ}{dt} \times \frac{1}{A \cdot C_0} \quad (\text{Eq. 2})$$

$$J_{ss} = C_0 \times P_{app} \quad (\text{Eq. 3})$$

dQ/dt is the steady-state appearance rate on the acceptor side of the skin. A is the area of the skin (CM²) and C_0 is the initial concentration of the drug in the donor phase. On the other hand, the cumulative permeated amount of SB through the skin after 48 h (Q_{48}) was calculated for all skin samples.

In-vivo UV-B protective experiments

-Animal care and treatment

The 6 to 7 week old female hairless mice used in this study were purchased from the laboratory animal center, Jundishapur University of Medical Sciences, Ahvaz, Iran. All animal experiments were carried out by the Ethical Committee of Ahvaz Jundishapur University of Medical Sciences (Approval number: N-9804). Mice were housed five per each cage and acclimatized for at least 1 week before the start of the experiment, and housed in the Animal Resource Facility of the Ahvaz Jundishapur University of medical sciences under the following conditions: 12 h dark/12 h light cycle, 24 °C temperature, and 10% relative humidity. The mice were fed a standard diet and water (Moghimpour et al. 2013).

- UVB irradiation protocol

The UVB irradiation was produced by Philips TL40W/12 RS lamp (Medical-Eindhoven, Holland) equipped with a UVB meter (Lutron Electronic, Taiwan) to regulate UV radiation dosage with a distance of 20 cm between the UVB lamp and the skin surface. The mice anesthetized by intraperitoneal injection of 90 mg/kg ketamine and 3 mg/kg xylazine and then received 600 mJ/cm² for 10 min, 5 times per week for 2 weeks.

– Hydrogel administration

Mice were randomly divided into 10 groups with 3-7 animals in each following groups: (1) Naïve (non-irradiated);(2) irradiated without treatment;(3) treated with blank hydrogel;(4) treated with the aqueous suspension of SB(100 µmol/L);(5) treated with hydrogel including SB(100µmol/L),(6) treated with hydrogel including SB (200 µmol/L);(7)treated with hydrogel including SB(250 µmol/L);(8) treated with hydrogel including SB (350 µmol/L); (9) treated

with hydrogel including SB(450 $\mu\text{mol/L}$) and (10) treated with Trademarke[®] Sun Screen (positive control). All groups were treated with 2mg/cm^3 of hydrogel or Trademarke[®] Sun Screen before UVB irradiation.

- **Histochemical Detection of H₂O₂-Producing Cells**

Immunohistochemical detection of H₂O₂ in all groups was done following a previously described procedure. 72 h after UVB irradiation or UVB irradiation plus hydrogel mice were euthanized and 6-cm-thick skin sections were incubated with 0.1 mol/L Tris-HCl buffer (pH 7.5), containing 1 mg/mL glucose and 1 mg/mL diaminobenzidine for 2 h at 37°C. Sections were then washed in distilled water and counterstained with methyl green and then identify H₂O₂ producing cell with a fluorescent microscope (Gonzage 2009).

- **Assay for Lipid Peroxidation products**

The epidermal microsomal fraction was used to determine the epidermal lipid peroxidation level using the thiobarbituric acid reaction method, as described previously (Sharma et al. 2007). 400 μM SB hydrogel and blank hydrogels were applied on the skin before UVB exposure and then 24 h after the UVB irradiation, mice were sacrificed and skin samples were collected. Briefly, 0.2 mL of the microsomal fraction was treated with 0.2 mL of 8.1% sodium dodecyl sulfate (SDS) and 3 mL thiobarbituric acid. The total volume was made up to 4 mL with distilled water and kept at 95 °C in a water bath for 1 h. The color was extracted with n-butanol. The absorbance was measured at 530 nm, and the resultant lipid peroxidation was expressed against control (normal skin).

- **Histologic evaluation of the skin**

For histologic evaluation, 72 h after UVB irradiation or UVB irradiation plus hydrogel, mice were euthanized and the skin tissues were fixed in 10% formaldehyde in 0.1M phosphate buffer (pH 7.4) overnight and fixed in paraffin. Sections were stained with hematoxylin-eosin and Masson's trichrome stain to identify collagen fibers and the inflammatory cellular response with 20× and 40× objectives. The thickness of the prickle cell layer was measured using an optical microscope (Olympus BX 51; Olympus).

- **Detection of pro-inflammatory cytokines in skin sections**

72 h after UVB irradiation or UVB irradiation plus hydrogel mice were euthanized and after the addition of phosphate-buffered saline, skin tissue samples were homogenized with a homogenizer (ULTRA-DISPERSER Type T25-S2; Janke & Kunkel GmbH & Co. KG IKA-Labortechnik) and an ultrasonic processor (Model VP-5 T; TAITEC) for a short time while cooling on ice, and samples were then centrifuged for 15min at 10000 × g at 4°C. The supernatant was stored at -70°C until use. IL-22 and TNF-α levels in the skin tissue were then quantitatively measured using ELISA kits (Endogen) with a detection limit of < 5 pg/mL (Maruyama et al. 2015).

Silibinin assay method

The determination of the amount of SB was carried out by HPLC with a C₁₈ column (Waters; 25 cm, 5 μm diameter) using a UV detector at 288 nm and methanol/water (80/20) as mobile phase

at a flow rate 1 ml/min. The limit of quantification (LOQ), accuracy, repeatability, and linearity were evaluated as method validation. The injection volume was 50 μ L.

Data analysis and statistics

All the experiments were repeated three times and data were expressed as the mean values. Statistical data were analyzed using the one-way analysis of variance (ANOVA) and $P < 0.05$ was considered to be significant with a 95 % confidence interval. To figure out the relationship between the dependent and independent variables, the simultaneous multi-regression test was used.

Results and Discussion

Validity of the drug measurement method

Regression analysis showed a significant relationship between concentration and area under the curve ($P = 0.001$) within the concentration range of 0.001-50 mg/ml and with a correlation coefficient of $R^2 = 0.999$. The LOQ was 0.001 mg/ml, and all reported concentrations were above this LOQ. The lack-of-fit, which appeared in the estimated absorbance changes, was not significant ($P = 0.116$). The accuracy of the assay method indicated the maximum difference between the reported concentration values and the actual values. The method showed the desired repeatability within and between days.

SB content and pH

The amounts of drug content in all hydrogels ranged from 97.5% to $101.6\% \pm 4.4\%$ (n=3). The pH values of the hydrogels ranged from 5-5.5. These values did not change during hydrogel storage.

Hydrogel spreadability

The spreadability results are shown in Table 1. The maximum spreadability was 10.5 cm, provided by Formulation 6. A significant correlation ($P = 0.029$) was found between % swelling and spreadability. This means that hydrogel spreadability is primarily affected by swelling properties.

Swelling properties of hydrogels

The swelling ratios recorded after 60 minutes for all hydrogels are presented in Table 1. Significant inverse ($P = 0.01$) and direct ($P = 0.014$) correlations were found between the swelling ratio and fucoidan and chitosan concentrations, respectively.

The maximum swelling ratio was provided by Formulation 3, which produced a high percentage of chitosan and a low percentage of fucoidan. The amount of water absorbed by a hydrogel is mainly dependent on hydrophilic groups in the chemical structure of the polymer, cross-linking density, and environmental conditions, such as pH (Ahmadi et al. 2015).

Chitosan is prepared by the partial deacetylation of chitin. Chitin has poor aqueous solubility because of the high number of acetylated groups and a rigid crystalline structure (Khor & Lim 2003). Therefore, chitosan that is prepared by the deacetylation of chitin demonstrates good

aqueous solubility (Murakami et al. 2010). Cross-linking the chitosan and glutaraldehyde decreases the aqueous solubility and increases the strength of the hydrogel.

Fucoidan is a sulfated polysaccharide with more hydrophilicity than chitosan. Unlike the hydrophilic nature of fucoidan, the lower swelling ratio was provided by hydrogels made with more fucoidan. This finding conflicts with what Sezer et al. found. They reported that the addition of fucoidan, which is more hydrophilic than chitosan, increased the swelling ratio of gels. It seems that hydrogel cross-linking with glutaraldehyde changed the swelling behavior in the present study. The swelling ratio is mainly dependent on hydrogel strength, and the hydrophilicity of the polymer did not show a strong impact on the swelling ratio. The swelling ratio provided in the present study after one hour is equal to the swelling ratio reported by Sezer et al. after six hours.

***In vitro* SB released from the hydrogel**

Percentages of cumulative SB released after 1 h and 48 h are presented in Table 1. According to these data, all hydrogels had a rapid release, with 18-26.5% of the drug released within the first hour. The highest and lowest release rates were reported for Formulations 3 and 9, respectively. On the other hand, 40-61% of the loaded drug was released within 48 h; the highest and lowest values in this regard were associated with Formulations 1 and 9, respectively.

Previously, it was reported that 80-90% of loaded SB in hydrogels based on pluronic 127 and caprolactone-polyethylene glycol released after 24 h (Makhmalzadeh et al. 2018). It seems that hydrogel based on chitosan-fucoidan released SB at a lower rate, indicating that it can act as a

sustained release carrier for topical delivery of SB. Sustained release carriers provide a release controlling system and possess a skin permeation controlling dosage form.

However, hydrogels generally release drugs at a sustained and slow rate. The percentage of fucoidan had a significant and reverse effect on the percentage of release after half an hour ($P = 0.036$) and 48 h ($P = 0.001$). This means that increasing the percentage of fucoidan reduces the drug release rate. However, the effect of chitosan percentage on release was not significant. Therefore, by changing the percentage of fucoidan, the desired release profile can be obtained.

The drug release kinetics were evaluated by fitting the release data to zero-order, first-order, Hixon-Crowell, and Higuchi models. The results showed that the Higuchi model ($R^2 = 0.974$) was the best for describing the mechanism of release. The Higuchi model is applied to describe the rate of drug release from a matrix (such as a hydrogel) such that the solvent causes the hydrogel to gradually swell and the concentration gradient is linear from the saturated concentration of the drug in the hydrogel matrix to the concentration at the hydrogel-dissolution medium interface (Mircioiu et al. 2019). Therefore, SB provided a saturated concentration in the hydrogel, and the release rate was mainly controlled by hydrogel swelling.

Insert Table 1

Optimized hydrogel composition and characterization

Based on the significant correlation between % chitosan and % fucoidan with swelling ratio and % R_1 , the optimized hydrogel should be made of 4% chitosan and 0.1% fucoidan. However, this hydrogel presented instability during storage, and for this reason, the optimized hydrogel was

made of 3% chitosan and 0.15% fucoidan. The characteristics of the optimized hydrogel, such as thermal behavior, rheology, morphology, FT-IR spectrum, *in vitro* drug release, permeability through normal and UV-treated mouse skin, and its *in vivo* sun protection efficacy, were evaluated.

- **DSC of optimized hydrogel**

The thermal behavior of the optimized hydrogel and pure SB in the heating program is illustrated in Fig 2. In this heating program, the SB and SB-containing hydrogel were heated to a temperature ranging from 0°C to 200°C, and the corresponding thermograms were prepared. SB has a melting point in the range of 164-174°C (Pooja et al. 2014), which is highly broadened in an optimum hydrogel thermogram. This indicates that the SB was homogeneously dispersed in the hydrogel, which might be due to the lower amount of SB in hydrogel compared to pure SB. Alternatively, it might be due to the low packing density of hydrogel as previously reported in silibinin-loaded nanoparticles (Sahibzada et al. 2017). The thermogram of the optimized hydrogel showed a major phase transition around 120°C that seemed to correspond to the ordered structure of chitosan-fucoidan hydrogel. Chitosan hydrogel demonstrated a glass transition temperature of around 130°C (Ray et al. 2010) that changed to an ordered structure in the chitosan-fucoidan hydrogel prepared in the present study. This ordered structure helps to release SB more quickly than low ordered hydrogels.

Insert Fig 2

Rheology of optimized hydrogel

The rheogram of the optimized hydrogel is shown in Fig 3. This hydrogel demonstrated shear thinning behavior and a Newtonian region at low values of the shear rate. It seems that the

chitosan-fucoidan interaction provided a high viscosity in the shear rate near zero, meaning that the aqueous phase did not flow at rest and the gel network was formed by chitosan and fucoidan.

Insert Fig 3

Evaluation of optimized hydrogel by FT-IR

Chitosan presents a band at 1559.17 cm^{-1} , which is assigned to the stretching vibration of the amino group of chitosan and 1333.5 cm^{-1} according to the vibration of C-H (de Souza et al. 2009). The disappearance of the 1595 cm^{-1} band in the hydrogel indicates cross-linked chitosan that results in the formation of gels (Fig 4). On the other hand, band 1240 cm^{-1} belonging to the fucoidan sulfate group has also disappeared, which seems to be involved in the gelation process as well. SB has three specific bands at 3457 (OH group), 2946 (CH group), and 1508 (aromatic ring) (Sezer et al. 2013), all of which disappeared in the hydrogel. This finding indicates that there is a bond between SB and hydrogel, which may be a reason for the relatively slow release of the drug.

Insert Fig 4

***In vitro* SB release through the optimized hydrogel**

The hydrogel contained 100, 250, and $450\text{ }\mu\text{mol/L}$ SB as demonstrated by the release profiles in Fig 5. The results indicated no significant difference ($P > 0.05$) between SB release profiles from hydrogels loaded with 100, 250, and $450\text{ }\mu\text{mol/L}$ SB. This means that SB concentration did not affect the release amount and mechanism. It seems that the SB in three hydrogels provided similar gradient concentrations. Based on this finding, the SB in three concentrations

demonstrated saturated solubility in hydrogels. The zero-order is the best model of SB release through hydrogels. It means that swelling may control SB release.

Insert Fig 5

-Permeability of SB loaded in optimized hydrogel through normal and UV-irradiated mouse skin

All skins were hydrated around 20-30% before the test was started. Therefore, all skins had a close degree of hydration. The thickness of the skin samples was $320 \pm 14 \mu\text{m}$. The permeability parameters, including flux and the cumulative permeated amount of SB after 48 h (Q₄₈), were calculated (Table 2). Previously, the J_{ss} of silibinin-loaded in PolyGel™ gel and Pluronic F127 gel through normal mouse skin were reported to be 0.8 and 0.25 $\mu\text{g}/\text{cm}^2 \text{ h}$, respectively (Makhmalzadeh et al. 2018). These values are comparable to the findings of the present study. Based on these findings, the following conclusions are presented:

- The penetration of irradiated skin increased compared to normal skin, indicating damage to the skin structure. UVB radiation is a well-known initiator of inflammation responses mediated by the skin that is associated with the production of reactive oxygen species (Ishida & Sakaguchi 2007). UVB decreases the expression of loricrin, involucrin, and filaggrin, which play an important role in the skin barrier (Kim et al. 2017). In another study, it was reported that the combination of UVB radiation and oxidative stress impaired the skin's molecular transport barrier after 5 h of radiation (Hernandez et al. 2019).

- Optimized hydrogel significantly reduced drug passage through the skin compared to the aqueous control. This reduction means that more of the drug stays in the skin. We found that 40-60% of loaded SB was released after 48 h through hydrogels. These values are greater than the values of Q48 provided by the optimized hydrogel through normal and UV-treated skins. This means that the rate of drug release is faster than the rate of SB permeability through different skins. Therefore, the drug release is not a rate-limiting step in SB permeability. Hydrogel decreased Q48 compared with the control when the skin's resistance and barrier against SB were strengthened. It seems that the hydrogel decreased SB skin permeability by increasing skin hydration and decreasing SB solubility in the skin.

SB, as a sun-protective substance, should stay on the epidermis to prevent sunlight from damaging the skin. It seems that the hydrogel has been able to retain silibinin in the skin. In a previous study, SB flux from rat skin was reported to be $0.43 \mu\text{g}/\text{cm}^2\cdot\text{h}$ (Pooja et al. 2014), which is in agreement with the results of this study.

Insert Table 2

Pathological results

The histological changes in different skin sections affected by UVB are presented in Fig 6. The first notable change was the increase in the thickness of the epidermis due to the proliferation of spiny cells called acanthosis. Also, hyperkeratosis (increased keratin layers) was another change that was visible on the surface of the epidermis. Within the epidermis, cells with wrinkled, dark, and cytoplasmic nuclei are more abundant than other lateral cells called sunburn cells. In the dermis, the infiltration of inflammatory cells with hyperemia and disruption of collagen fibers was also observed. Dermal blood vessel dilation and vascular hyper-permeability were also found.

These changes were previously reported in psoriasis lesions (Katayama 2018) and UVB-treated skin (Sharma & Katiyar 2010). These changes were also observed in groups receiving blank hydrogel and a positive control group.

In the treatment group with the optimized hydrogel, epidermal hyperplasia, vascular hyper-permeability, erythema, cutaneous edema, and other changes induced by UVB irradiation were reduced in a dose-dependent manner. In these groups, the lowest change was observed in the group treated with 450 μM /L SB. Skin thickness and sunburn cell count in different groups when evaluated at 24 h after UVB exposure are presented in Fig 5. UVB irradiation increased skin thickness compared to normal skin. All UVB-irradiated skin treated with different formulations decreased skin thickness compared to UVB-irradiated untreated skin.

No significant difference was found between the thickness of UVB-irradiated skin treated with blank hydrogel, hydrogel containing 100 μM SB, and 100 μM aqueous suspension of SB. This means that blank hydrogel demonstrated a protective effect against UVB irradiation damage. No significant difference was found between the skin thickness in normal skin and irradiated skin treated with a hydrogel containing 450 μM . In a previous study, hydrogel containing SB-loaded pomegranate oil-based nanocapsules exhibited anti-inflammatory effects on skin damage induced by UVB radiation in mice (Marchiori et al. 2017). They reported that 1 mg/ml SB loaded in hydrogel (around 2000 μM) reduced the skin thickness by 64-79% when compared to irradiated skin. In the present study, 450- μM SB decreased skin thickness by 100% when compared to irradiated skin. It seems that hydrogel composed of chitosan and fucoidan fortified the SB as a UVB-protective agent. Normal skin structure was observed in the control group. According to obtained results, the optimal hydrogel has been able to prevent the harmful effects

of UV-B light on the skin while preventing the morphological changes of the skin due to UVB irradiation dose-dependently.

Insert Fig 6

Determination of lipid oxidation products

Microsomal lipid fractions were used to evaluate lipid peroxidation in the epidermis. One of the symptoms of UVB-induced oxidative stress is lipid peroxidation. The UV absorption values that are a sign of lipid peroxidation were determined in different groups. UV absorption in irradiated skin treated with 450 μ M SB-loaded hydrogel was 0.15 ± 0.01 , which was significantly lower than untreated irradiated skin (UV absorption: 1.66 ± 0.13). Irradiated treated skin with blank hydrogel demonstrated UV absorption of 0.68 ± 0.04 , which was significantly lower than untreated irradiated skin.

H₂O₂ production in UVB-irradiated skins

H₂O₂ production was determined as a marker of oxidative stress in the skin after UVB irradiation. To demonstrate that the UVB-induced infiltration of leukocytes was a major source of oxidative stress, we localized H₂O₂-producing cells via an immunostaining process (Fig 7). As shown by the immunostaining, UVB-induced infiltrating cells are the major source of H₂O₂ production. H₂O₂ cells were seen in both the epidermis and dermis by dark spots. These H₂O₂ cells were not observed in normal skin, and UVB irradiated skin was treated by 450 μ M SB hydrogels.

The SB-loaded hydrogel inhibited oxidative stress and production of H₂O₂, as well as total reactive oxygen species (ROS) by epidermal cells, which activate various cell signaling pathways. This intercellular signaling plays an important role in cell growth, differentiation, and proliferation, which can lead to skin cancer (Pal et al. 2015).

Insert Fig 7

SB hydrogel inhibits UVB-induced inflammation

Recent studies have illustrated the pathogenic role of IL-22, a cytokine produced by NK and CD4⁺ cells in skin disease. IL-22 was increased in human keratinocytes after UVB radiation and promoted keratinocyte proliferation and cytokine production during UVB-induced skin inflammation (Kim et al. 2017). TNF- α secretion from UVB-irradiated keratinocytes and fibroblasts was reported. Not only is TNF- α associated with epidermal and systemic inflammatory responses, but it also promotes apoptosis, lymphocyte activation, and hyperproliferation skin disorders (Bashir et al. 2009). Therefore, TNF- α and IL-22 were measured to evaluate the protective effect of SB hydrogel against skin damage induced by UVB.

UVB promoted the levels of TNF- α and IL-22 significantly ($P < 0.05$) when compared to non-irradiated skin (Fig 8). Applying the 450- μ M SB hydrogel decreased the levels of TNF- α and IL-22 when compared to irradiated untreated skin. The level of IL-22 in irradiated skin treated with SB hydrogel did not show a significant difference with non-irradiated skin. Blank hydrogels decreased the levels of TNF- α and IL-22 by more than 40% when compared with irradiated untreated skin. Therefore, SB demonstrated very potent anti-inflammatory effects and can inhibit damage due to UVB irradiation.

The anti-inflammatory effect of SB is affected by its carrier. In a previous study, 2000 $\mu\text{mol/L}$ of SB was loaded in nanocapsules and dispersed into the hydrogel reduced mouse ear edema and leukocyte infiltration induced by UVB 24 h after treatment (Marchiori et al. 2017). However, SB loaded in chitosan-fucoidan hydrogel demonstrated anti-inflammatory effects with a lower concentration (450 $\mu\text{mol/L}$), perhaps due to the anti-inflammatory effect of the blank chitosan-fucoidan hydrogel.

Insert Fig 8

Conclusion

The mixture of chitosan and fucoidan is a suitable base for hydrogel preparation, as it demonstrated a UVB-protective effect and favored drug storage and spread on the skin. SB exhibited UVB-protective, anti-inflammatory, and antioxidant effects. Therefore, loading chitosan-fucoidan hydrogel with SB can produce a protective formulation that can prevent keratinocyte proliferation and differentiation, inflammation in the epidermis by decreasing inflammation mediators, such as TNF- α and IL-22. Overall, SB can be developed as a natural chemopreventive agent that can be used for the treatment of UVB-induced skin inflammation. Hydrogels composed of chitosan and fucoidan with chemopreventive effects can boost the UVB-protective effect of SB.

Compliance with Ethical Standards

-Conflicts of Interest

The authors declare that they have no conflict of interest.

- Statement of Human and Animal Rights

The animal studies were performed after receiving approval of the Institutional Animal Care and Use Committee in Ahvaz Jundishapur University of Medical Sciences (Approval number: N-9804).

References

- Ahmadi F, Oveisi Z, MohammadiSamani S, Amoozegar Z (2015) Chitosan based hydrogel: characteristics and pharmaceutical applications. *Res Pharm Sci* 10 (1): 1-16.
- Badek KH (2000) Evaluation of properties microcrystalline chitosan as a drug carrier, Part I. *In vitro* release of diclofenac from microcrystalline chitosan hydrogel. *Acta Pol Pharm* 57 (6): 431-440.
- Bashir MM, Sharma MR, Werth VP (2009) UVB and proinflammatory cytokines synergistically activate TNF- α production in keratinocytes through enhanced gene transcription. *J Invest Dermatol* 129 (4): 994-1001.
- Bhattarai N, Gunn J, Zhang M (2010) Chitosan-based hydrogels for controlled, localized drug delivery. *Advanced drug delivery reviews* 62(1):83-99.
- Baviskar DT, Biranwar YA, Bare KR., et al (2013) *In vitro* and *In vivo* evaluation of diclofenac sodium gel prepared with cellulose ether and carbopol 934P. *Trop J Pharm Res* 12(4): 485-489.

- Cavinato M, Waltenberger B, Baraldo G, Grade CVC, Stuppner H, Hansen-Durr P (2017) *Plant extracts and natural compounds used against UVB-induced photoaging*. *Biogerontology*, **18**(4): 499-516.
- Cuomo F, Cofelice M, Lopez F (2019) Rheological characterization of hydrogels from alginate-based nanodispersion. *Polymers*; 11 (2), 259, doi.org/10.3390/polymer 11020259.
- Dai YN, Li P, Zhang JP, Wang AQ, Wei Q (2008) swelling characteristics and drug delivery properties of nifedipine-loaded pH-sensitive alginate-chitosan hydrogel beads. *J Biomed Mater Res B Appl Biomater* 86 B (2): 493-500.
- Davies DJ, Ward RJ, Heylons JR (2014) Multi-species assessment of electrical resistance as a skin integrity marker for in vivo percutaneous absorption studies. *Toxicol in Vitro*; 18: 351-358.
- de Souza Costa-Junior E, Pereira MM, Mansure HS (2009). Properties and biocompatibility of chitosan films modified by blending with PVA and chemically cross-linked. *J Mater Sci Mater Med* 20; 553-61.
- Gu M, Dhanalakshmi S, Singh RP, Agarwal R (2005) Dietary feeding of silibinin prevents early biomarkers of UVB radiation-induced carcinogenesis in SKH-1 hairless mouse epidermis. *Cancer Epidemiol Prevent Biomark* 14(5):1344-9.
- Gonzaga ER (2009) Role of UV light in photodamage, skin aging, and skin cancer. *Am J Clin Dermatol* 10(1):19-24.
- Hernandez AR, Vallejo B, Ruzgas T, Bjorklund S (2019) The effect of UVB irradiation and oxidative stress on the skin barrier. A new method to evaluate sun protection factor based on electrical impedance spectroscopy. *Sensors* 2376; doi: 10.3390/s 19102376.
- Katayama H (2018) Development of psoriasis by continuous neutrophil infiltration into the epidermis. *Exp Dermatol* 27(10): 1084-1091.

- Khor E, Lim LY (2003) Implantable application of chitin and chitosan. *Biomater* 24: 2339-2349.
- Kim S, Jang JE, Kim J, Lee Y, Lee DW, Yong Song S., et al (2017) Enhanced barrier function and anti-inflammatory effect of cultured coconut extract on human skin. *Food Chem Toxicol* 106: 367-375.
- Kim Y, Lee J, Choi CW, Hwang Y, Seung Kang J., et al (2017) the pathogenic role of IL-22 and its receptors during UVB-induced skin inflammation. *PLOS ONE* 30; 1-15.; doi.org/10.1371/journal.pone.0178567.
- Ishida T, Sakaguchi I (2007) Protection of human keratinocytes from UVB-induced inflammation using root extract of lithospermumerythrorrhizon. *Biol Pharm Bull* 30: 928-934.
- Makhmalzadeh BS, Molavi O, Vakili MR, Zhang H-F, Solimani A, Abyaneh HS, et al (2018) Functionalized Caprolactone-Polyethylene Glycol Based Thermo-Responsive Hydrogels of Silibinin for the Treatment of Malignant Melanoma. *J Pharm PharmSci* 21(1):143-59.
- Maruyama H, Tamauchi H, Kawakami F, Yoshinaga K, Nakano T (2015) Suppressive effect of dietary fucoidan on proinflammatory immune response and MMP-1 expression in UVB-irradiated mouse skin. *Planta Medica* 81(15):1370-4.
- Marchiori MCL, Rigon C, Camponogara C, Oliveira SM, Cruz L (2017) Hydrogel containing silibinin-loaded pomegranate oil-based nanocapsules exhibits anti-inflammatory effects on skin damage UVB radiation-induced in mice. *J PhotochemPhotobiol B: Biology* 170:25-32.

- Mircioiu C, Voicu V, Anuta V., et al (2019) mathematical modeling of release kinetics from supramolecular drug delivery systems. *Pharmaceutics* 11, 140; doi: 10.3390/pharmaceutics11030140.
- Moghimipour E, Salimi A, Sharif MakhmalZadeh B (2013) Effect of various solvents on the *in vitro* permeability of vitamin B12 through excised rat skin. *Trop J Pharm Res.* 12(5):671-7.
- Mohamed MA, Jung M, Lee SM, Kim J (2014) Protective effect of *Disporum sessile* D. Donextract against UVB-induced photoaging via suppressing MMP-1 expression and collagen degradation in human skin cells. *J PhotochemPhotobiol B: Biology* **133**: 73-79.
- Moon HJ, Lee SR, Shim SN, Jeong SH, Stonik VA, Rasskazov VA, et al (2008) Fucoidan inhibits UVB-induced MMP-1 expression in human skin fibroblasts. *Biol and Pharm Bull* 31(2):284-9.
- Murakami K, Aoki H, Nakamura S, Nakamura S, Takikawa M, Hanzawa M., et al (2010) Hydrogel blends of chitin/chitosan, fucoidan and alginate as healing-impaired wound dressing. *Biomater* 31: 83-90.
- Pal HC, Athar M, Elmes CA, Afag F (2015) Fiestin inhibits UVB-induced cutaneous inflammation and activation of PA3K/AKT/NFkB signaling pathways in SKH-1 hairless mice. *PhotochemPhotobiol* 91(1): 225-234.
- Pooja D, Bikkina DJB, Kulhari H, Nikhila N, Chinde S, Raghavendra Y, et al (2014) Fabrication, characterization and bio evaluation of silibinin loaded chitosan nanoparticles. *Int J BiolMacromol* 69:267-73.

- Qiu Y, Park K (2001) Environment-sensitive hydrogels for drug delivery. *Adv Drug Deliv Rev* 53: 321-339.
- Rao N, Rao KP, Muthalik S (2009) Clinical studies and antimicrobial activity of ciprofloxacin hydrochloride mediated dental gels for periodontal infection. *Asian J Pharmacol*; 3: 125-134.
- Ray M, Pal K, Anis A, Banthia AK., et al (2010) Development and characterization of chitosan-based polymeric hydrogel membranes. *Designed Monomers Polymers*; 13: 193-206.
- Sahibzada M, Sadiq A, Khan S., et al (2017) Fabrication, characterization and *in vitro* evaluation of silibinin nanoparticles: an attempt to enhance its oral bioavailability. *Drug Des Devel Ther*; 11: 1453-464.
- Sezer AD, Cevher E, Hatipoğlu F, Oğurtan Z, Baş AL, Akbuğa J (2008) Preparation of fucoidan-chitosan hydrogel and its application as burn healing accelerator on rabbits. *Biol Pharm Bull* 31(12):2326-33.
- Sharma SD, Katiyar SK (2010) Dietary grape seed proanthocyanidins inhibit UVB-induced cyclooxygenase-2 expression and other inflammatory mediators in UVB exposed and skin tumors of SKH-1 hairless mice. *Pharm Res* 27: 1092-1102.
- Sharma SD, Meeran SM, Katiyar SK (2007) Dietary grape seed proanthocyanidins inhibit UVB-induced oxidative stress and activation of mitogen-activated protein kinases and nuclear factor- κ B signaling *in vivo* SKH-1 hairless mice. *Mol Cancer Therapy* 6(3):995-1005.
- Zhao T, Maniglio D, Chen J, Chen B, Migliaresi C (2016) Development of pH-sensitive self-nano emulsifying drug delivery systems for acid-labile lipophilic drugs. *Chem Phys lipids* 196:81-8.

Table 1. the composition and properties of hydrogels prepared based on the factorial design (mean±SD, N=5)

formulaNo.	% chitosan	% fucoïdan	% Swelling (60)	% R ₁	% R48	Spreadability (cm)
1	1	0.1	23.5±3.1	25.2±1.6	60.9 ± 3.3	4.67±0.5
2	2	0.1	124.2±9.4	24.1±1.9	56.7 ± 4.5	8.7±0.66
3	4	0.1	132.3±11.3	26.9±0.9	58.1±4.2	9.8±1.1
4	1	0.2	52.4±5.3	20.3±0.7	49.3±3.8	6.2±0.33
5	2	0.2	60.7±4.8	19.3±1.1	47.8±5.1	6.7±0.40
6	4	0.2	119±7.5	24.6±0.9	50.1±3.3	10.5±0.75
7	1	0.4	29.6±3.4	20.1±0.6	43.7±4.4	5.2±0.42
8	2	0.4	39.2±2.2	21.9±1.2	44.1±2.8	5.5±0.51
9	4	0.4	70.6±8.5	18.2±0.8	40.7±4.4	7.1±0.53

Table 2. SB permeability parameters through normal and UVB-Irradiated skins after topical application of optimized hydrogel and SB aqueous control (Mean \pm SD, N= 5)

Skin Type	Flux ($\mu\text{g}/\text{cm}^2 \cdot \text{h}$)	Q 48 ($\mu\text{g}/\text{cm}^2$)	P-value
Normal skin treated by optimized hydrogel	0.4 \pm 0.01	21 \pm 1	0.03 [*]
Irradiated skin treated by optimized hydrogel	0.6 \pm 0.01	29 \pm 2	-
Normal skin treated by aqueous control	0.7 \pm 0.02	34 \pm 3	0.042 ^{**}
Irradiated skin treated by aqueous control	0.78 \pm 0.02	38 \pm 4	0.035 ^{**} *

*, **, ***: Irradiated skin treated by optimized hydrogel compared with: Normal skin treated by optimized hydrogel, Normal skin treated by aqueous control, Irradiated skin treated by aqueous control, respectively.

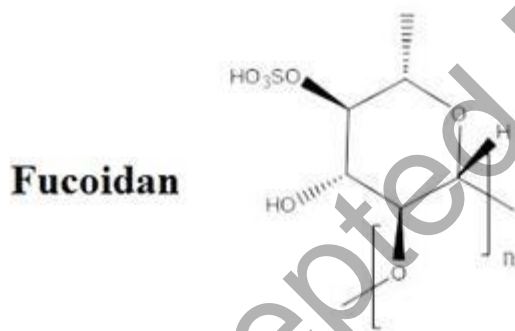
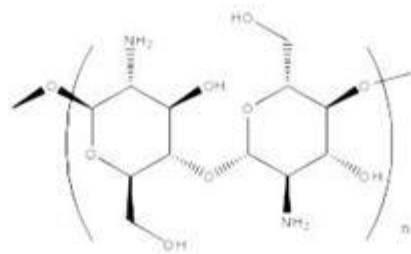
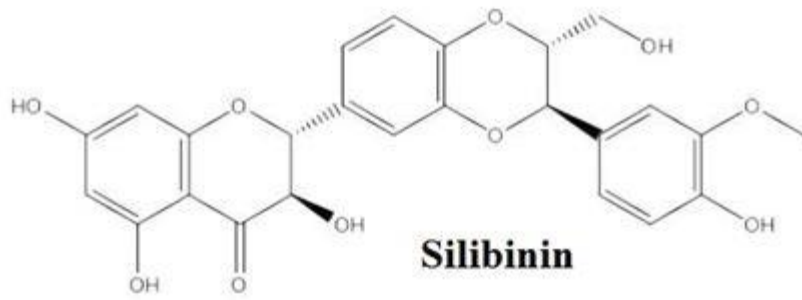


Figure 1. The chemical structure of Silibinin, chitosan, and fucoidan

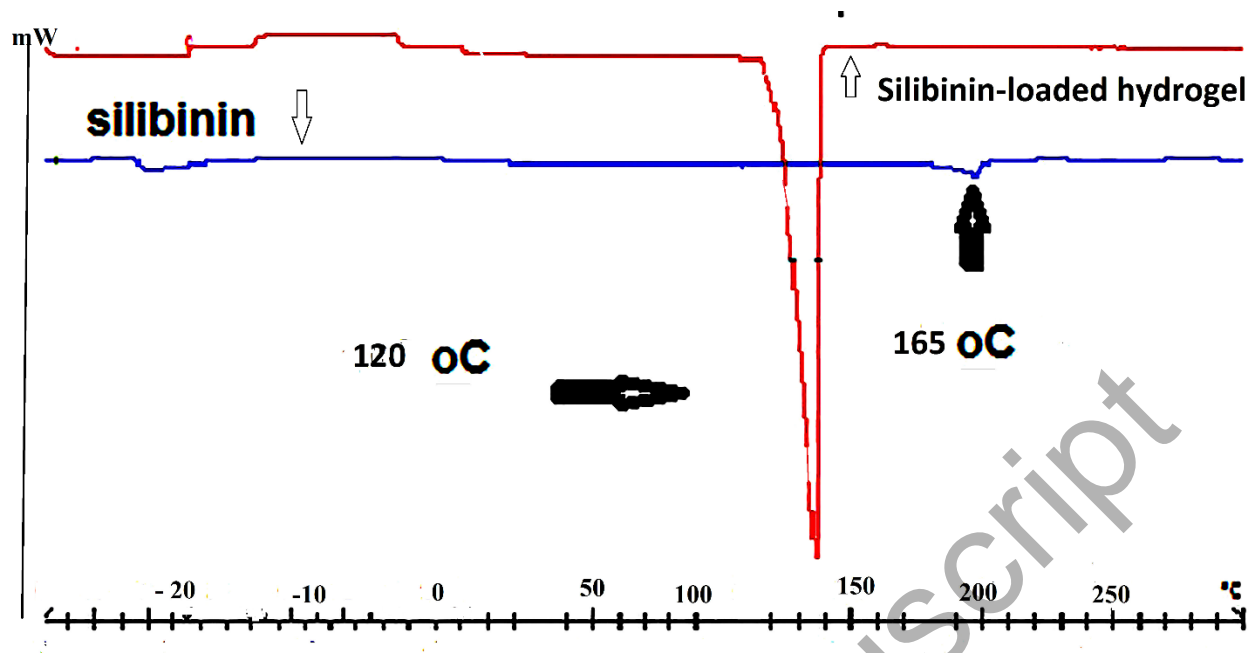


Figure 2. Thermograms of SB, and SB-loaded hydrogel obtained in the heating program

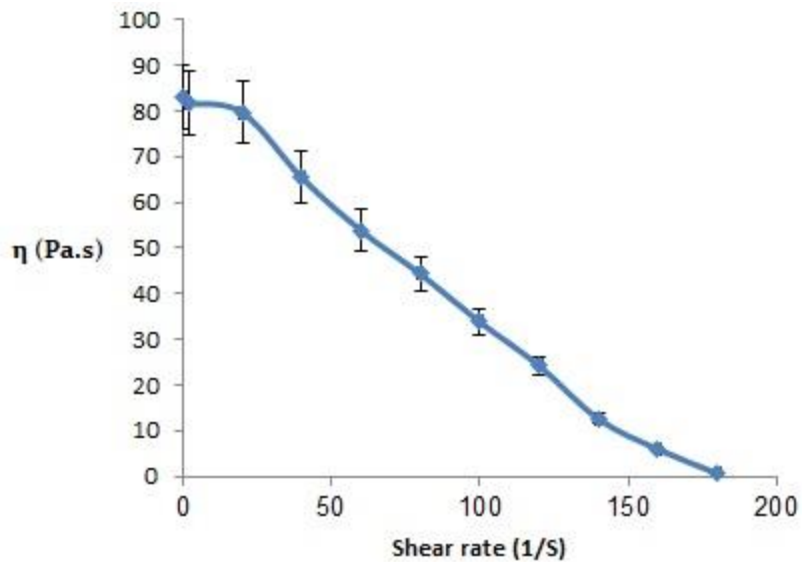


Fig 3. The shear rate-viscosity curve of optimized hydrogel

Accepted Manuscript

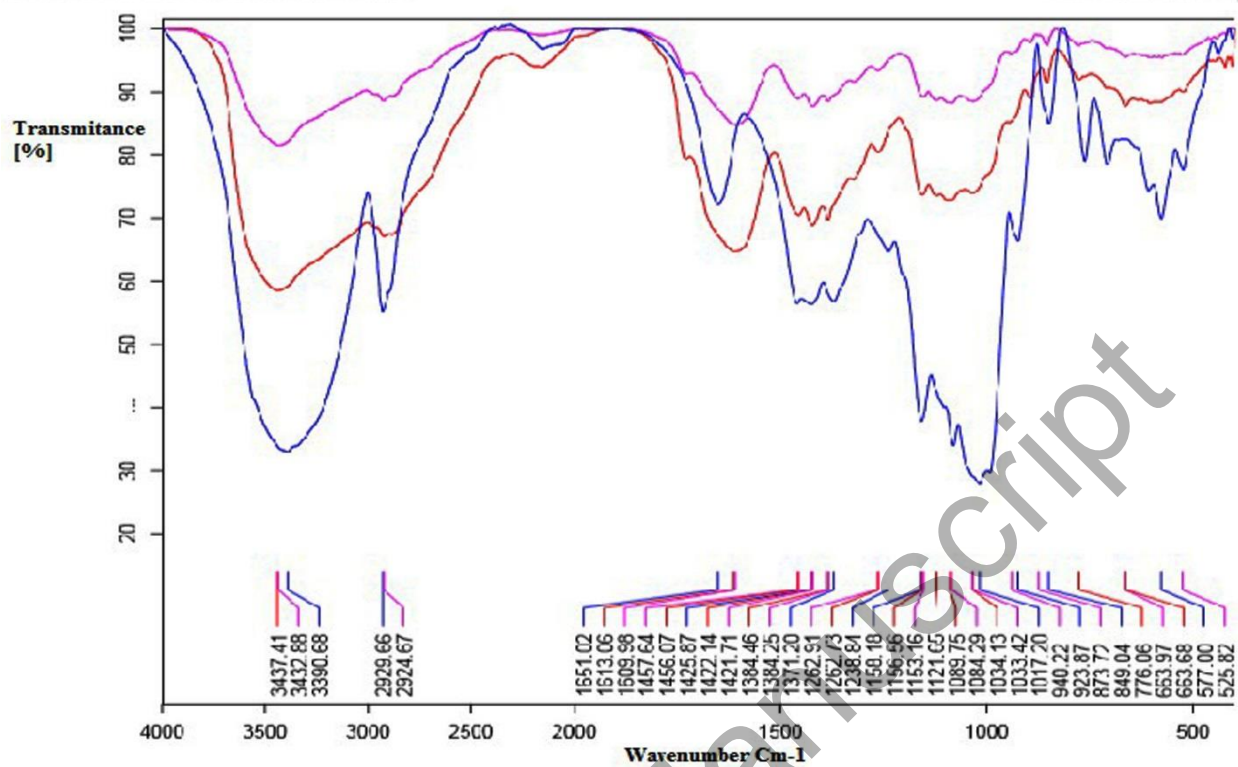


Figure 4. The FT-IR spectrum of fucoidan (blue) –blank hydrogel (red) -hydrogel with silibinin (purple)

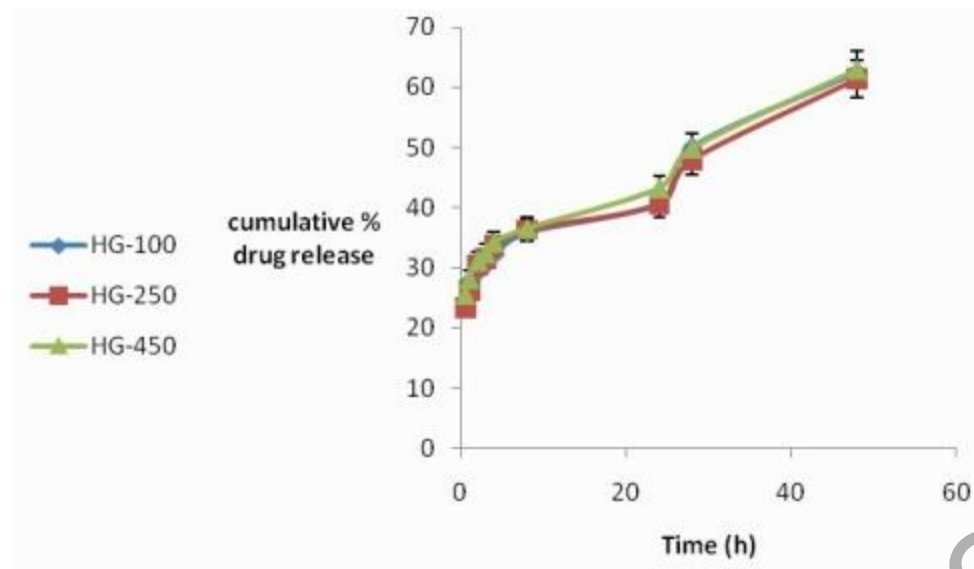
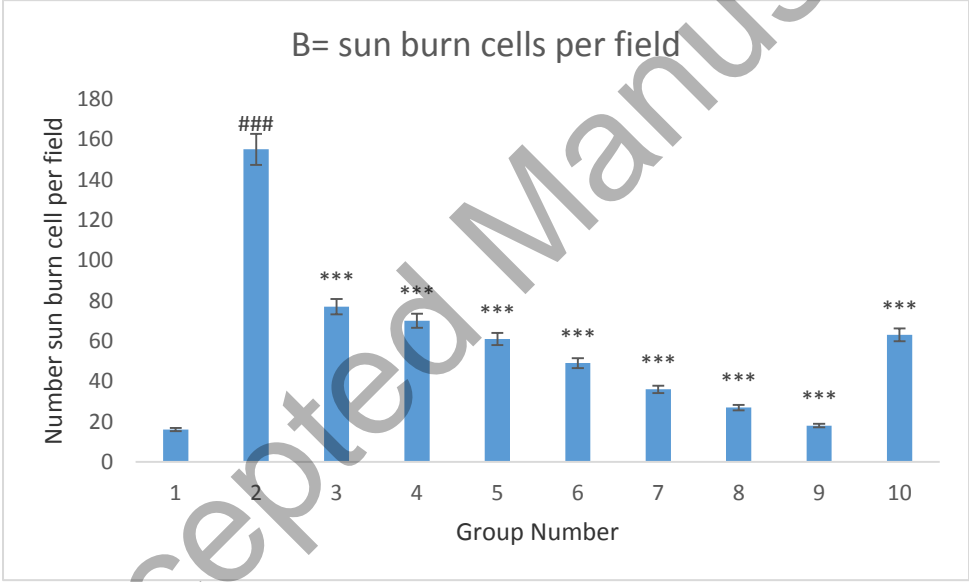
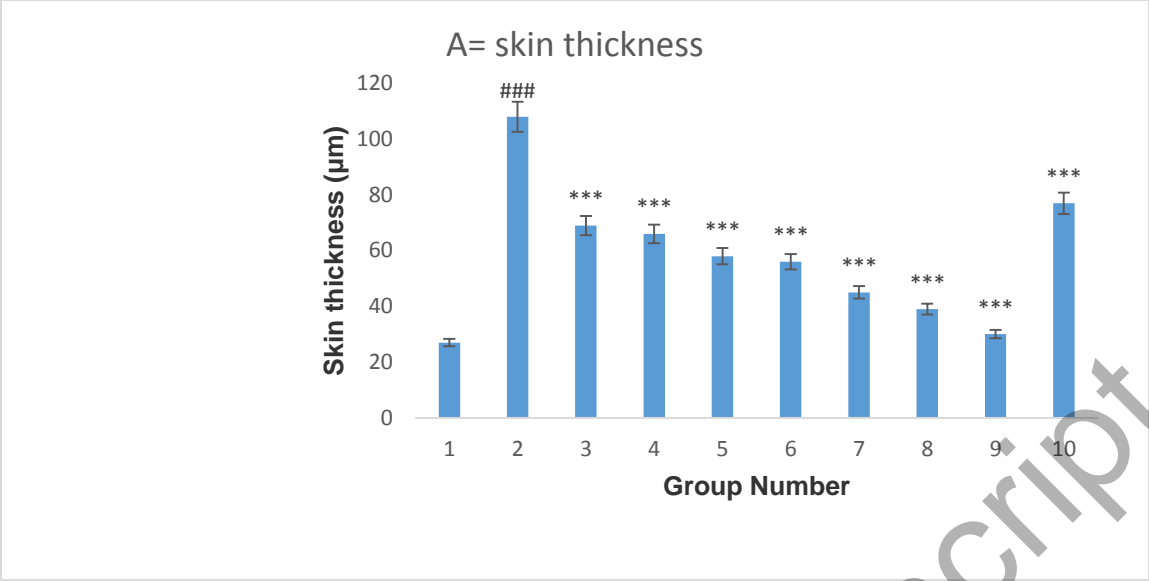


Figure 5. the release profiles of SB-loaded in hydrogel with three different concentrations (n=5)

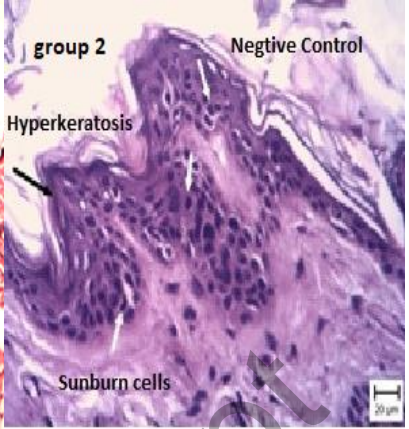
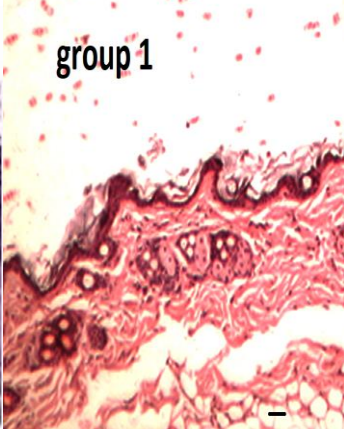
HG-100: 100 μmol/L SB loaded hydrogel

HG-100: 250 μmol/L SB loaded hydrogel

HG-100: 450 μmol/L SB loaded hydrogel

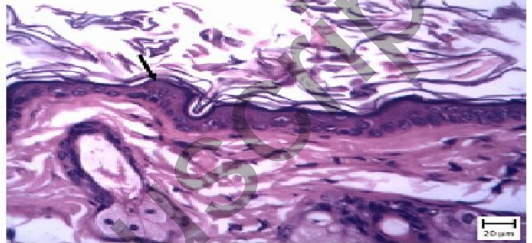
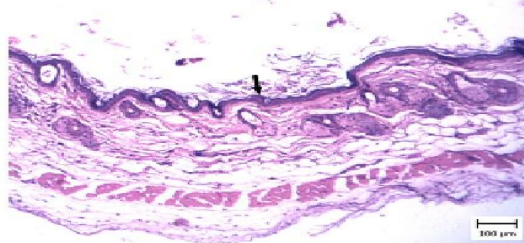


C: Histological images

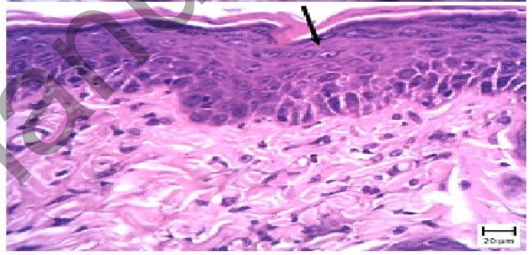
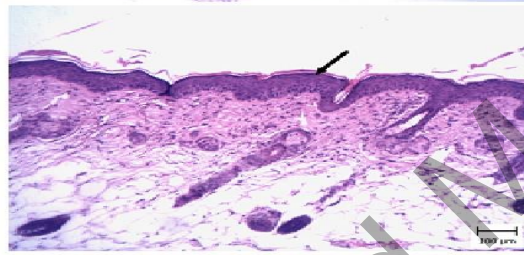


Negative Control

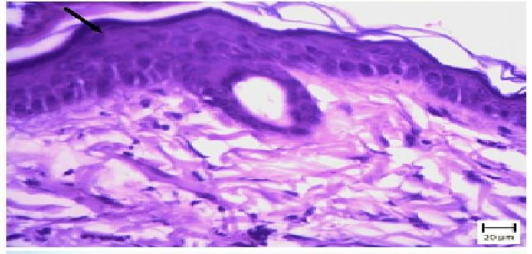
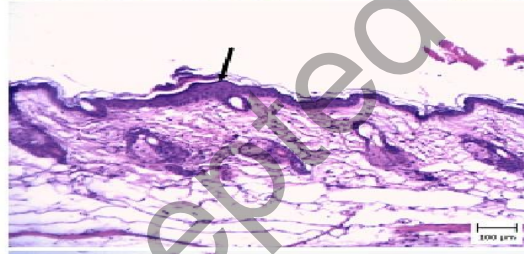
100



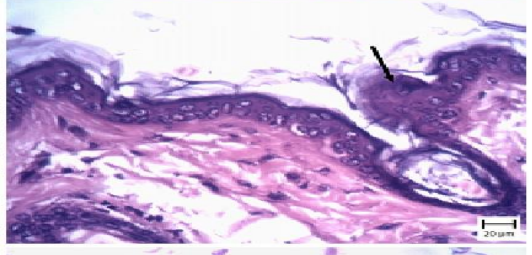
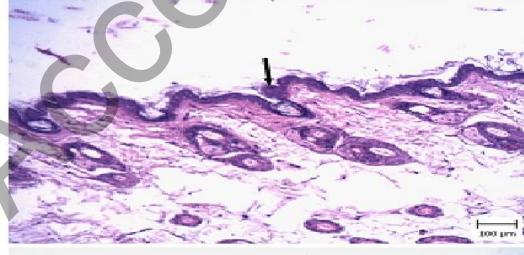
200



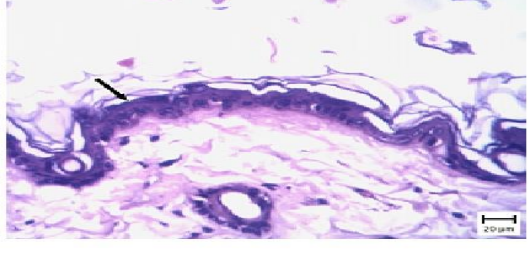
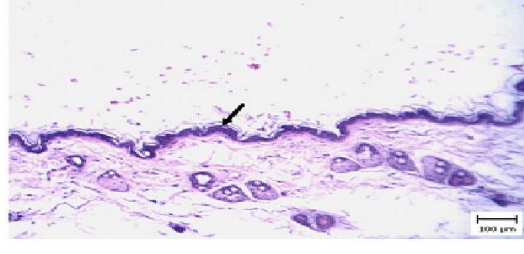
250



350



450



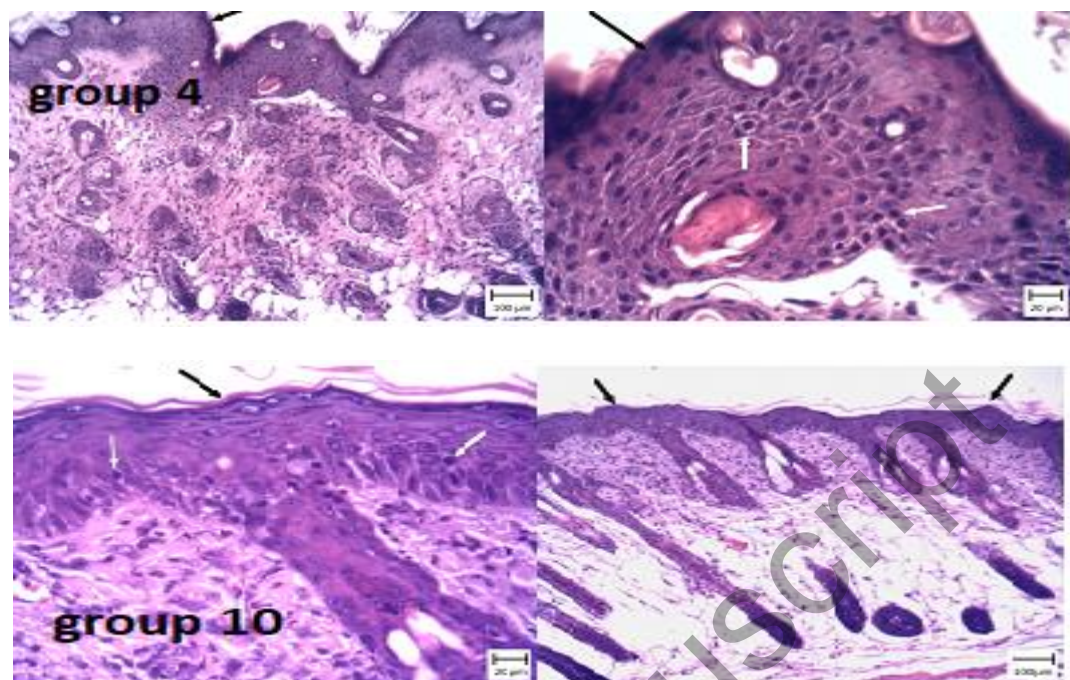


Figure 6. Protective effects of different groups on UVB irradiation-induced skin injury, A: Skin thickness ; B: Number of sunburn cells per field, C: Histological images. 10 mg/cm² of all formulations were applied before UVB expose to the skin and the skin thickness and sunburn cells were measured 24 h after the UVB irradiation; ### p<0.001 when compared with the normal un-irradiated skin (group 1), * p<0.05, ** p<0.01, and *** p<0.001 when compared with the untreated irradiated group (group 2). 1: Normal un-irradiated skin, 2: untreated irradiated skin, 3: irradiated skin treated by blank hydrogel, 4: irradiated skin treated by 100 µM SB aqueous suspension, 5: irradiated skin treated by 100 µM SB hydrogel, 6: irradiated skin treated by 200 µM SB hydrogel, 7: irradiated skin treated by 250 µM SB hydrogel, 8: irradiated skin treated by 350 µM SB hydrogel, 9: irradiated skin treated by 450 µM SB hydrogel, and 10: irradiated skin treated by Trademark sunscreen (positive control)

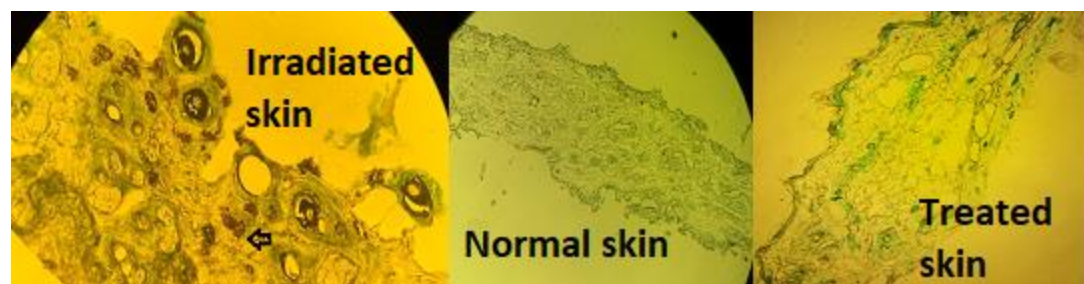


Figure 7.The production of H_2O_2 in different skins

Accepted Manuscript

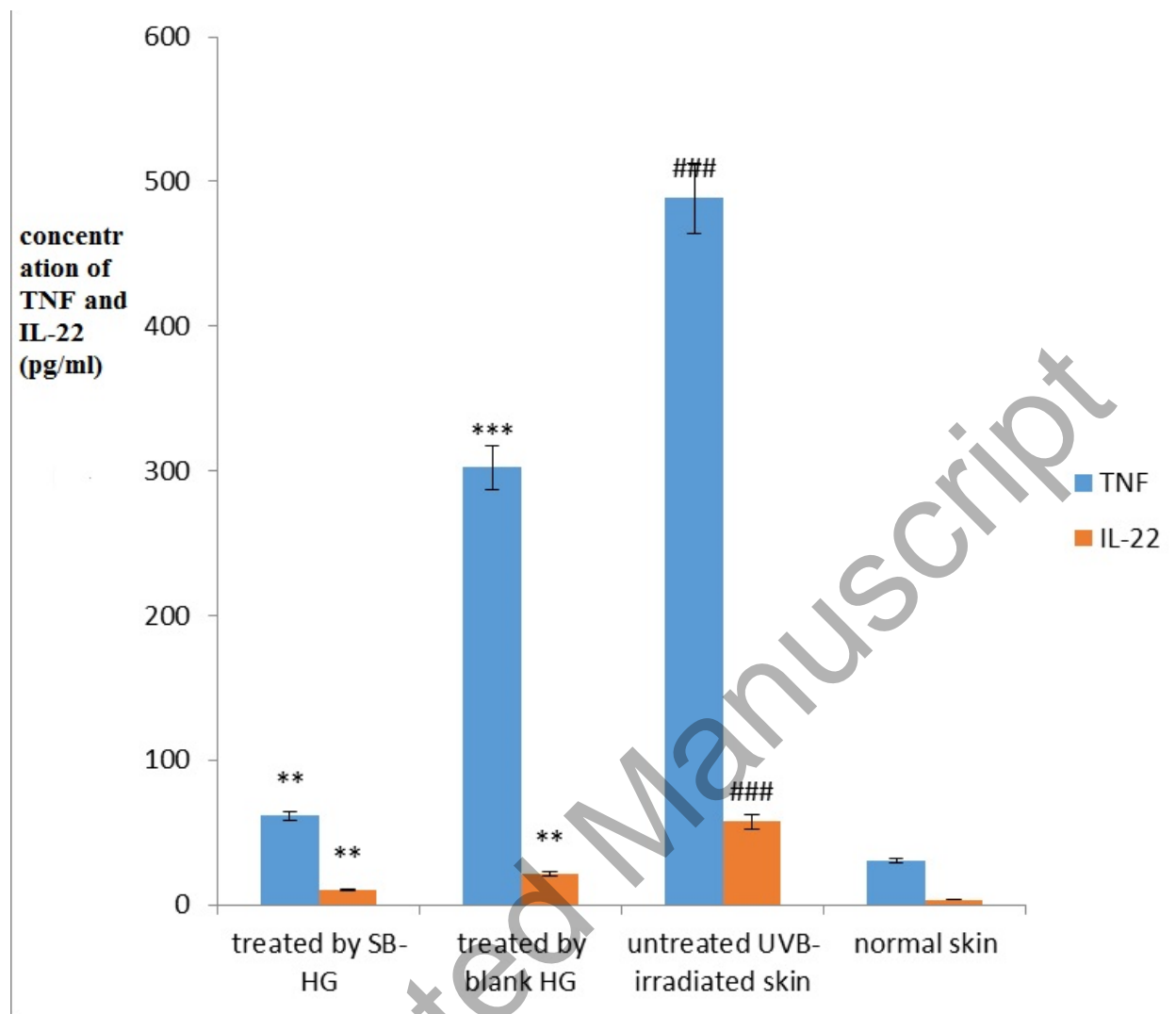


Figure 8. The levels of TNF- α , and IL-22 in different skins. ### p<0.001 when compared with the normal un-irradiated skin (group 1), * p<0.05, ** p<0.01, and *** p<0.001 when compared with the untreated irradiated group (the number of replicates was 4)